Rayleigh-Taylor instability in magnetohydrodynamics with finite resistivity in a horizontal magnetic field

Y. B. Sun ,[*] J. N. Gou, C. Y. Cao, and C. Wang
State Key Laboratory of Explosion Science and Technology, Beijing Institute of Technology, Beijing 100081, China

R. H. Zeng
Fujian Key Laboratory of Wind Disasters and Wind Engineering, Xiamen University of Technology, Xiamen 361024, China

(Received 5 June 2023; accepted 16 November 2023; published 13 December 2023)

Recent studies have revealed the significant influence of finite resistivity on high-energy-density plasmas, contrary to the previous findings of Jukes [J. Fluid Mech. **16**, 177 (1963)]. This paper reexamines Jukes' theory in the context of magneto-Rayleigh-Taylor instability in magnetohydrodynamics with finite resistivity represented by η. The inadequacy of Jukes' approach due to an erroneous boundary condition is demonstrated, and it is shown that although the theory provides some physical insights, it fails to capture crucial features. The dispersion relation proposed in this study highlights that larger growth rates tend to diffuse the magnetic field rapidly, negating its suppressive effect. Moreover, the Atwood number has a significant influence on the growth-rate curves' shape, which differs from those of viscous or elastic flows and ideal magnetohydrodynamics. Additionally, long wavelengths grow proportionally to $\eta^{1/3}$, while α indicating growth rates behaves classically when the magnetic field is entirely diffused.

DOI: 10.1103/PhysRevE.108.065208

I. INTRODUCTION

The Rayleigh-Taylor (RT) instability, a phenomenon in fluid dynamics, commonly arises at interfaces between fluids or materials exhibiting different densities. It has extensive applications across numerous scientific domains. Notably, recent comprehensive surveys conducted by Zhou and colleagues have shed light on these applications [1–4].

An extension of the Rayleigh-Taylor (RT) instability that incorporates the presence of a magnetic field is known as the magneto-Rayleigh-Taylor (MRT) instability. Its significance spans a broad range of physics, encompassing astrophysics and inertial confinement fusion [5–9]. Numerous experiments and numerical simulations have demonstrated that using an insulated magnetic field to decrease thermal conductivity losses and guide fast electrons to enhance the fusion yield in magnetized laser-driven implosions poses a significant threat to magnetized linear inertial fusion due to the MRT instability [10–17]. The role of magnetic fields in this context can be ambiguous. On one hand, strong magnetic fields can mitigate hydrodynamic instabilities by means of magnetic tension. On the other hand, the MRT instability is exacerbated by the suppression of thermal conduction in the presence of a magnetic field [18–20]. Magnetohydrodynamic instabilities are also present in such implosions [21]. Nonlinear analyses reveal that a magnetic field can suppress perturbation growth rates due to the magneto-Richtmyer-Meshkov (MRM) and MRT instabilities [22–24]. An analytical method can elucidate the effects of a magnetic field, with the transverse magnetic field entirely suppressing the seeded wavelength below a critical value (λ_c), while a vertical magnetic field suppresses the perturbation less. However, most studies limited to ideal magnetohydrodynamics neglect the diffusion of magnetic fields [18].

Recent experiments on high-energy-density plasmas [25,26] have shown that the magnetohydrodynamic equations must include finite resistivity for the design of future experiments, and the widely used Lee-More model may also underestimate plasma conductivity in high-energy-density regimes [27], while the Spitzer model is strictly valid for fully ionized plasmas with low density and high temperature [28]. Manuel *et al.* demonstrated that the Lee-More resistivity model is insufficient in the regime of interest to explain the experimental results and that the eV, Mbar plasmas must have a lower resistivity than expected [25–27]. To address these issues, an experiment has been proposed to measure resistivity and improve the mathematical modeling [29–31]. It has been proposed that the assumption of infinite electrical conductivity for a fluid, besides neglecting other dissipative processes, can result in significant discrepancies between idealized magnetohydrodynamics theoretical predictions and experimental results. For example, the magneto-Kelvin-Helmholtz instability, which is initially stable under magnetic field suppression, can become unstable and grow exponentially and periodically due to finite resistivity [32].

Viscosity plays a significant role in suppressing the growth rate of the MRT instability, which has recently attracted special attention in inertial confinement fusion [33,34] and in astrophysics [35]. Weber *et al.* discovered that a turbulent kinetic-energy cascade was produced by the hot spot when plasma viscosity was not considered. However, when

[*]sunyb@bit.edu.cn

the hot-spot Reynolds number falls between 10 and 100, small-scale mixing is dampened by viscosity [33,34]. Hydrodynamic instability was observed in high-energy-density plasma experiments at the National Ignition Facility and at Omega lasers facility [36,37]. A theoretical examination indicates that the most unstable wavelength derived from MRT instability by considering viscosity is compatible with astrophysical observations [35]. Finite resistivity may be the primary focus while studying the MRT instability in magnetized plasmas as fluid viscosity does not alter behavior at short wavelengths, which are more strongly affected by finite resistivity [38]. Walsh *et al.* performed detailed numerical simulations to demonstrate that resistive diffusion will reduce the effectiveness of tension stabilization for short wavelengths and long timescales [39]. Moreover, for the nonlinear ablative RT instability, the interface becomes more unstable by the thermal conduction suppression effects and by the existence of magnetic fields self-generated by the Biermann battery mechanism [40,41].

Detailed analyses of the dependence of the MRT instability on finite resistivity in magnetohydrodynamics were first made by Jukes [42]. However, a careful examination of his derivations reveals that an erroneous boundary condition was used in the continuity of the magnetic stress, resulting in incorrect dispersion relations. Jukes' derivation is included here for illustration, as it occurs in infinite-conductivity theory where there is a finite skin current of vanishing thickness, and the product of current density and thickness remains finite. At $z = 0$, the continuity equation takes the form

$$\Delta(\rho D u_y) = \frac{gk^2}{n^2}(\rho_1 - \rho_2)u_y(0), \tag{1}$$

where k is the perturbed wave number, g is the acceleration due to gravity, ρ is the density of the plasma at the interface, and $u_y(0)$ is the perturbed velocity at the interface with $y = 0$. However, according to Chandrasekhar's theory [18], the continuity expression along the vertical direction is obtained by integrating the momentum equation across the interface, which should include the magnetic field. Therefore, the boundary condition should be

$$\Delta(\rho D u_y) + \frac{\mu_0 H^2 k^2}{n^2}\Delta(D u_y) = \frac{gk^2}{n^2}(\rho_1 - \rho_2)u_y(0). \tag{2}$$

The validity of Eq. (2) can be attributed to the presence of a horizontal magnetizing field H, which furnishes a surface-tension-like force to stabilize the interface. Noted that the stabilizing effect of the magnetic field only impacts the MRT instability growth for perturbed modes parallel to the magnetic field [39,43]. It is imperative to incorporate this force explicitly in the boundary condition to obtain an accurate description of the system under consideration. Jukes' initial investigation into the MRT instability in magnetohydrodynamics, however, overlooked the impact of a horizontal magnetic field, leading to an erroneous conclusion. To rectify this, one must use Eq. (2) instead of Eq. (1) while formulating the boundary conditions, as it provides the correct dispersion relation. The revised expression encompasses various phenomena of interest resulting from arbitrary Atwood number, resistivities, and wavelengths.

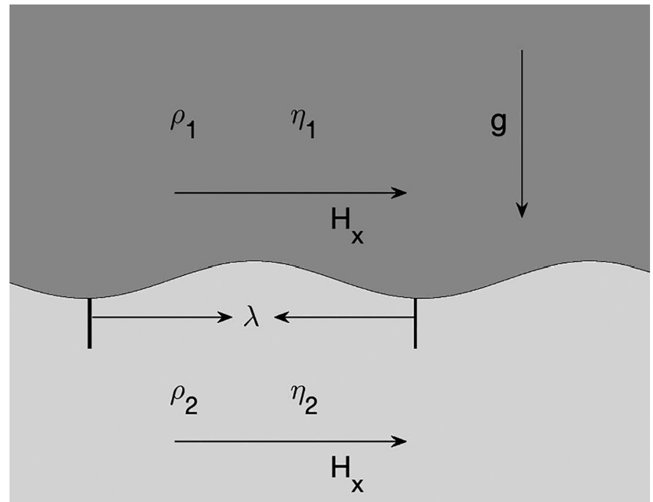

FIG. 1. Diagram of perturbed interface in magnetohydrodynamics.

In this paper, we present a study of the magneto-Rayleigh-Taylor (MRT) instability in magnetohydrodynamics with finite resistivity. The governing equations are briefly described in Sec. II. The dependence of the growth rates on physical parameters of interest is discussed in Sec. III. Finally, the conclusions and remarks are presented in Sec. IV.

II. PHYSICAL MODEL AND MATHEMATICS

Consider a partially conducting fluid of density ρ_1 and resistivity η_1 occupying the half space $0 < z < \infty$ and supported by another conducting fluid of density ρ_2 and resistivity η_2 occupying the half space $-\infty < z < 0$. Both fluids are placed in a horizontal magnetic field $\mathbf{H} = (H_x, 0, 0)$ and a vertical gravitational field $\mathbf{g} = (0, 0, g)$, as shown in Fig. 1. The equilibrium fluid pressure P, which satisfies the hydrostatic equation $\rho\mathbf{g} = \nabla P$, is assumed to be always positive and to support the fluid.

The relevant equations governing the incompressibility and momentum in both flows require

$$\nabla \cdot \mathbf{u} = \mathbf{0}, \tag{3}$$

$$\rho\frac{\partial \mathbf{u}}{\partial t} = -\nabla P + \rho\mathbf{g} + \mu_0 \mathbf{J} \times \mathbf{H}, \tag{4}$$

where $\mathbf{u}$ is the perturbed velocity along the x and z directions, P is the pressure, $\mathbf{J}$ is the electric-current density, and μ_0 is the magnetic permeability. It is well known that the instabilities in compressible fluids behave very much like the incompressible theory to assure the validity of Eq. (3) [44]. Moreover, to keep the mathematics simple, throughout this paper, the effects of the heat flow are neglected. To complete the derivations of the perturbed magnetic field strength due to the perturbation on the interface, we introduce Maxwell's equations with the displacement currents neglected, which read

$$\nabla \cdot \mathbf{H} = \mathbf{0}, \tag{5}$$

$$\nabla \times \mathbf{H} = \mathbf{J}, \tag{6}$$

$$\nabla \times \mathbf{E} = -\mu_0\frac{\partial \mathbf{H}}{\partial t}, \tag{7}$$

where $\mathbf{E}$ is the intensity of the electric field. Note that, for a moving medium, the electric field should be

$$\mathbf{J} = \sigma(\mathbf{E} + \mu_0 \mathbf{u} \times \mathbf{H}), \tag{8}$$

where σ is the conductivity of the plasma. The detailed derivations of the perturbed magnetic fields and the decay modes can be found in the Appendix. Next, our focus shifts to the continuity equations in order to establish the dispersion relations for the MRT instability considering finite resistivity.

First, continuity of the velocity along the z direction requires

$$kA_1 - kB_1 + kA_2 + kB_2 = 0. \tag{9}$$

We derive the corresponding Maxwell's stress tensor to realize the requirements of the continuities of stress tensors $T_{ixz} = H_x h_{iz}$. According to their definitions along the x direction, we have

$$H_x h_{1z} = H_x h_{2z}. \tag{10}$$

Substituting Eqs. (A6) and (A8) into Eq. (A2) and using the fact that Eq. (10) must hold for all z and about the perturbed magnetic fields along the y direction, we have the following expressions:

$$h_{1z} = \left[\frac{H_x k^2}{n} A_1 e^{-kz} + \frac{H_x k^2}{\frac{\eta_1}{\mu_0}(q_1^2 - k^2) - n} B_1 e^{-q_1 z}\right] \sin kx, \tag{11}$$

$$h_{2z} = \left[-\frac{H_x k^2}{n} A_2 e^{kz} + \frac{H_x k^2}{\frac{\eta_2}{\mu_0}(q_2^2 - k^2) - n} B_2 e^{q_2 z}\right] \sin kx. \tag{12}$$

Therefore, substituting Eq. (A9) into Eqs. (11) and (12), we have

$$\frac{H_x k^2}{n} A_1 + \frac{\rho_1 n}{\mu_0 H_x} B_1 + \frac{H_x k^2}{n} A_2 - \frac{\rho_2 n}{\mu_0 H_x} B_2 = 0. \tag{13}$$

Based on the expression of Maxwell's stress tensor along the z direction, we then have

$$T_{izz} = -H_x h_{ix}, \tag{14}$$

which is alternatively written as

$$h_{1x} = h_{2x}. \tag{15}$$

By using the same procedures for deriving Eqs. (11) and (12), we have

$$h_{1x} = \left[-\frac{H_x k^2}{n} A_1 e^{-kz} - \frac{H_x q_1 k}{\frac{\eta_1}{\mu_0}(q_1^2 - k^2) - n} B_1 e^{-q_1 z}\right] \cos kx, \tag{16}$$

$$h_{2x} = \left[-\frac{H_x k^2}{n} A_2 e^{kz} + \frac{H_x q_2 k}{\frac{\eta_2}{\mu_0}(q_2^2 - k^2) - n} B_2 e^{q_2 z}\right] \cos kx. \tag{17}$$

Similarly, we can also obtain

$$-\frac{H_x k^2}{n} A_1 - \frac{\rho_1 n}{\mu_0 H_x} \frac{q_1}{k} B_1 + \frac{H_x k^2}{n} A_2 - \frac{\rho_2 n}{\mu_0 H_x} \frac{q_2}{k} B_2 = 0. \tag{18}$$

We now need to obtain the stress tensor based on Eq. (A11). Before doing so, we first express the pressure on the perturbed surface from Eq. (4), which gives

$$\begin{aligned} P_1 &= P_0 - \left(\rho_1 n + \frac{\rho_1 g k}{n}\right) A_1 + \left(\rho_1 n \frac{k}{q_1} + \frac{\rho_1 g k}{n}\right) B_1 + \frac{u_0 {H_x}^2 B_1}{\frac{\eta_1}{u_0}(q_1^2 - k^2) - n}\left(k q_1 - \frac{k^3}{q_1}\right), \\ P_2 &= P_0 - \left(\rho_2 - \frac{\rho_2 g k}{n}\right) A_2 - \left(\rho_2 n \frac{k}{q_2} - \frac{\rho_2 g k}{n}\right) B_2 + \frac{u_0 {H_x}^2 B_2}{\frac{\eta_2}{u_0}(q_2^2 - k^2) - n}\left(\frac{k^3}{q_2} - k q_2\right). \end{aligned} \tag{19}$$

Finally, we have the equation for the continuity of stress tensor along y direction S_{izz}, and it reads as

$$-P - H_x h_{1x} = -P - H_x h_{2x}. \tag{20}$$

At the perturbed interface, the expression of the perturbed magnetic field h_{ix} can be simplified as follows:

$$h_{1x} = -\frac{H_x k^2}{n} A_1 - \frac{H_x q_1 k}{\frac{\eta_1}{\mu_0}(q_1^2 - k^2) - n} B_1 = -\frac{H_x k^2}{n} A_1 - \frac{\rho_1 n}{\mu_0 H_x} \frac{q_1}{k} B_1, \tag{21}$$

and

$$h_{2x} = -\frac{H_x k^2}{n} A_2 + \frac{H_x q_2 k}{\frac{\eta_2}{u_0}(q_2^2 - k^2) - n} B_2 = -\frac{H_x k^2}{n} A_2 - \frac{\rho_2 n}{\mu_0 H_x} \frac{q_2}{k} B_2. \tag{22}$$

Based on Eqs. (21) and (22), the fourth stress condition described by Eq. (20) can be shown as follows:

$$\left(\rho_1 n + \frac{\rho_1 g k}{n} + \frac{k^2 H_x^2}{n}\right) A_1 - \frac{\rho_1 g k}{n} B_1 - \left(\rho_2 n - \frac{\rho_2 g k}{n} + \frac{k^2 H_x^2}{n}\right) A_2 + \frac{\rho_2 g k}{n} B_2 = 0. \tag{23}$$

Actually based on Eq. (14), the contributions of magnetic terms $H_x h_{ix}$ on both sides of the perturbed interface remain equivalent.

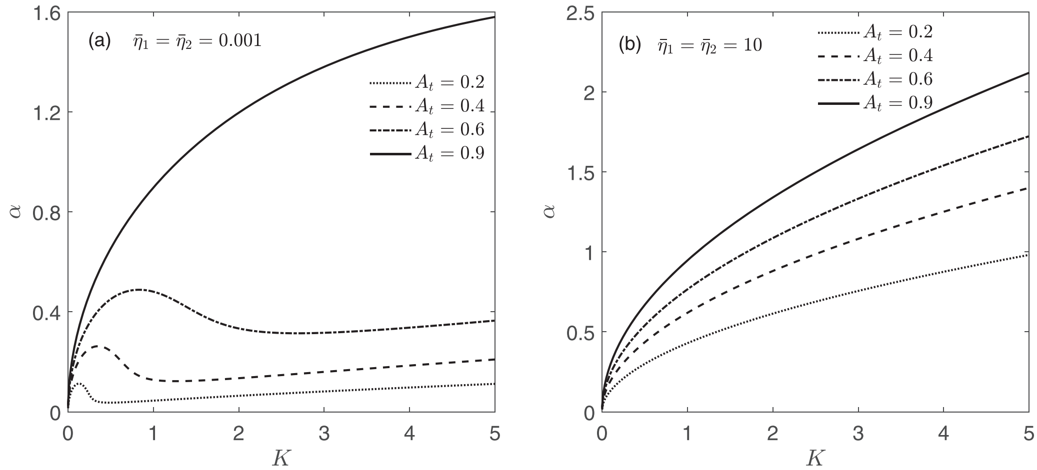

FIG. 2. Growth rates α as a function of K for different values of A_t, with (a) $\bar{\eta}_1 = \bar{\eta}_2 = 0.001$ and (b) $\bar{\eta}_1 = \bar{\eta}_2 = 10$, where $\alpha = nV/g$, $K = kV^2/g$, $V = (\mu_0 H_x{}^2/\rho_2)^{1/2}$, and $\bar{\eta}_i = \eta_i g/V^3$.

These four equations including Eqs. (9), (13), (18), and (23) are linear and homogeneous in A_1, B_1, A_2, and B_2. They have nontrivial solutions if and only if the determinant of the coefficient vanishes. Therefore, we have the dispersion relations

$$\left[(\rho_1+\rho_2)n^2-(\rho_1-\rho_2)gk+2\mu_0 H_x{}^2k^2\right]\left[\frac{\rho_2 n^2\frac{m_2}{k}+\mu_0 H_x{}^2k^2}{\rho_2 n^2+\mu_0 H_x{}^2k^2}+\frac{\rho_1 n^2\frac{m_1}{k}+\mu_0 H_x{}^2k^2}{\rho_1 n^2+\mu_0 H_x{}^2k^2}\right]-4\mu_0 H_x{}^2k^2=0. \tag{24}$$

Jukes derived the dispersion relation for the MRT instability in this case but only considered a partially conducting fluid above the interface [42], which renders the following simplified dispersion relation,

$$(\rho_1+\rho_2)n^2\left(\frac{m}{k}+1\right)+(\rho_1-\rho_2)(m+k)g-2\left(1-\frac{\rho_2}{\rho_1}\right)\frac{gk^3B_x^2}{n^2}-2k^2B_x^2\left(\frac{m}{k}+\frac{\rho_2}{\rho_1}\right)=0, \tag{25}$$

where $B_x = \mu_0 H_x$. In contrast, for the given continuity condition involving the stress tensor along the z direction, Jukes only considered the pressure and gravity forces along with the vertical displacement, which reads

$$P_1 + \rho_1 g\xi = P_2 + \rho_2 g\xi, \tag{26}$$

where ξ is the perturbed amplitude. Nevertheless, Jukes ignored the magnetic stress acting on the perturbed interface,

$$T_{izz} = -B_x b_{ix}, \tag{27}$$

which leads to the inconsistency with the dispersion relation presented herein.

III. DISCUSSIONS

A. Effect of Atwood number

Figure 2(a) describes the variations of the perturbed growth rates α as a function of the dimensionless wave number K. α increases monotonically to the maximum value, and then decreases gradually. However, after achieving the minimum growth rates, α then grows linearly when $A_t = 0.2$. The curves for $A_t = 0.4$ and $A_t = 0.6$ follow those for $A_t = 0.2$. However, when $A_t = 0.9$, in contrast with the previous cases, α increases monotonically with the increasing wave number because the decay mode m_i depends strongly on the growth rates n, as shown in Eq. (A9). In this case, the interface is essentially unaffected by the magnetic field because the magnetic field is totally diffused by the resistivity. Note that, for the smallest wave numbers, the growth rates of the instability are similar to the classical dispersion relation

$$n^2 = A_T kg, \tag{28}$$

which is consistent with the fact that the growth rates are rather insensitive to the details of the velocity fields. By including a horizontal magnetic field, the dispersion relation becomes

$$n^2 = A_T kg - 2\frac{\mu_0 H_x^2}{\rho_1+\rho_2}k^2, \tag{29}$$

which indicates that perturbations with wavelengths less than λ_c are totally stabilized. λ_c is

$$\lambda_c = 4\pi\frac{\mu_0 H_x^2}{(\rho_1-\rho_2)g}. \tag{30}$$

The horizontal magnetizing field causes the clearly decreasing trends. For the perturbation with small η and A_t, the horizontal magnetic field strongly affects the instability and significantly suppresses the perturbation with high wave numbers, as shown in Eq. (29), in which case the curves with $A_t = 0.2$ behave like those of the MRT instability with infinite conductivity. However, for wavelengths longer than λ_c in the ideal magnetohydrodynamics, the interface is totally stabilized.

Figure 2(b) plots the variations of the growth rates with dimensionless resistivity $\bar{\eta}_1 = \bar{\eta}_2 = 10$. The magnetic

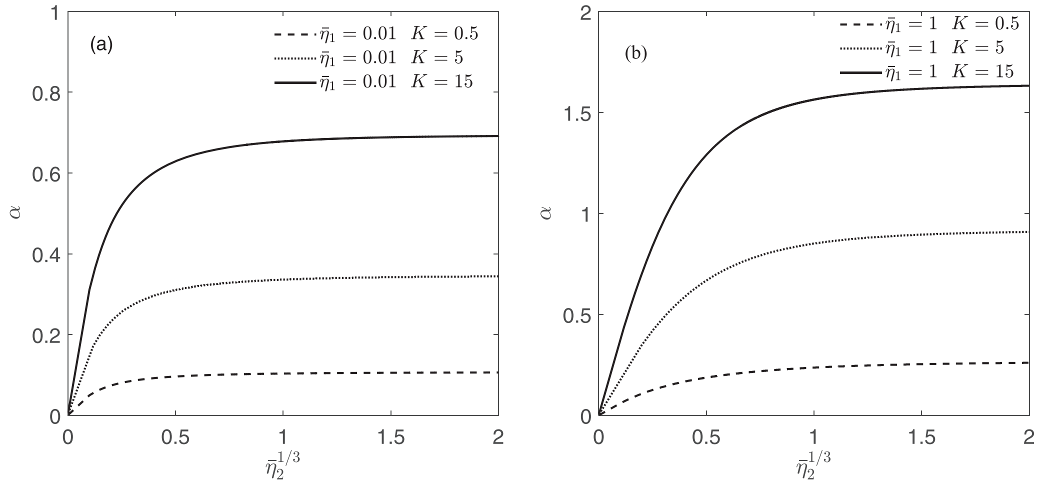

FIG. 3. Growth rates α as a function of K for $\bar{\eta}_1 = 0.01$ and different K, with (a) $A_t = 0.2$ and (b) $A_t = 0.9$, where $\alpha = nV/g$, $K = kV^2/g$, $V = (\mu_0 {H_x}^2/\rho_2)^{1/2}$, and $\bar{\eta}_i = \eta_i g/\mu_0 V^3$.

diffusion induced by a larger resistivity can strongly decrease the magnetic stress tensor and thus destabilize the interface. Thus, the magnetic stabilization of the MRT instability would be significantly reduced. Unexpectedly, these curves become almost identical to the classical curves produced by Eq. (28), which demonstrates that the suppression due to a horizontal magnetic field entirely vanishes, which is consistent with the numerical simulations [29,30]. However, it cannot be inferred from Jukes' theory.

B. Effects of electrical resistivity

One of the interesting phenomena observed by Jukes is that the perturbations with moderately long wavelengths grow rapidly at a rate $\alpha \propto \eta^{1/3}$, as shown in Fig. 3. This growth rate is also numerically verified in magnetized high-energy-density plasmas [30], for which the Lee-More model significantly underestimates the electrical conductivity for plasmas in the eV, Mbar regime [25]. Specifically, we investigate herein how long wavelengths grow at the rate $\alpha \propto \eta^{1/3}$ when the resistivity is not large. In addition, after the dimensionless resistivity increases to $\bar{\eta} \approx 1$, α tends to reach a constant that depends strongly on K. This phenomenon is again confirmed by the fact that the magnetic field in the plasma with resistivity η_2 is strongly diffused and the other plasma with $\eta_1 = 0.01$ contributes more to suppress the growth rate, as shown in Fig. 3(a). However, with $\eta_1 = 1$, as shown in Fig. 3(b), α quickly grows to almost recover the classical growth rate in ideal fluids shown as Eq. (28) because the magnetic field on both sides is diffused by larger resistivities and the suppressive effects of the magnetic field disappear.

C. Effects of resistivity ratio

In the context of inertial confinement fusion plasmas, recent numerical simulations reveal that the MRT instability is not directly impacted by the electrical resistivity but rather by the growth of the magnetic field. Furthermore, computations based on the Lee-More model exhibit a loss of suppressive effects for finite-conductivity plasmas [29]. Figure 4 shows how resistivity affects the growth rates of the MRT instability in the presence of a horizontal magnetic field. For the smallest wave number K, the growth rates of the perturbation with varying $\bar{\eta}$ retain essentially identical values. Since the growth rates are independent of the resistivity of the plasmas and of the horizontal magnetic field, the results resemble the classical results of a RT instability in ideal fluids shown in Eq. (28). The growth rates behave differently for the larger wave number K: They become dominated by the joint effects of the resistivity and the horizontal magnetic field and are proportional to K at high orders of K.

Figure 4(a) shows that, for the perturbed system with $A_t = 0.2$, the growth rates are enhanced by the incremental resistivity, particularly for high wave numbers. The separate horizontal magnetic field suppresses the growth rate of the RT instability and stabilizes the perturbed interface below the critical wavelength. For ideal magnetohydrodynamics, the magnetic flux tubes move with the fluids and therefore would be bent by the vorticity, generating the magnetic stress tensor acting on the perturbed interface [29,42]. However, for nonzero resistivity, the damping current induced by the resistivity causes the magnetic field to diffuse away from the disturbed interface, which weakens the magnetic-field intensity and thus weakens the inhibition effect.

Similarly, when $\bar{\eta} = 0.001$, the perturbed growth rate first increases to the maximum value and then decreases gradually to give rise to a linear relation between α and K. As $\bar{\eta}$ varies from 0.1 to 10, the growth rate increases monotonically, which differs from the aforementioned perturbation with $\bar{\eta} = 0.001$. In these cases, the resistivity significantly diffuses the horizontal magnetic field, thereby destroying the stabilizing mechanism and leading to the growth rate shown in Fig. 4(b), which is almost the same as the classical growth rates.

D. Comparison of Jukes' results with those of the present theory

Figure 5 shows the growth rates given by Jukes and those obtained in this work when $A_t = 0.9$: Jukes' theory and the proposed method yield different growth rates. Combined with

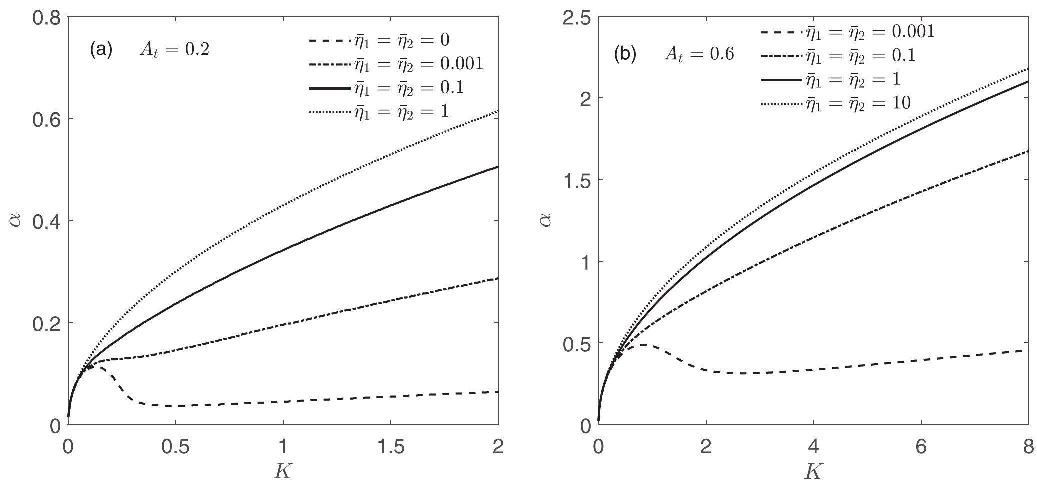

FIG. 4. Growth rates α as a function of K for different values of $\bar{\eta}$, with (a) $A_t = 0.2$ and (b) $A_t = 0.6$, where $\alpha = nV/g$, $K = kV^2/g$, $V = (\mu_0 {H_x}^2/\rho_2)^{1/2}$, and $\bar{\eta}_i = \eta_i g/V^3$.

the discussion in Sec. III A, our results reveal that, when $A_t = 0.9$, the growth rate increases monotonically as the wave number grows, in which case the magnetic field is diffused by a larger resistivity and does not suppress the disturbance of high wave number. Apparently, in contrast with our results, Jukes' theoretical growth rates remain similar to those obtained with small A_t. The diffusion effect of the resistivity on the magnetic field also depends on the growth rate, as shown in Eq. (A9). With sufficiently large growth rates, even a small resistivity can dampen the inhibition effect of the magnetic field on instability. However, Jukes' theory does not reveal this interesting insight.

According to Jukes' dispersion relation, the growth rates are given as a function of $\eta_2^{1/3}$ in Fig. 5(b), which reveals that, for moderately long wavelengths, the analytical growth rate depends on resistivity η as $\alpha \propto \eta^{1/3}$. By comparing the growth rates with Fig. 3, our results show that, for small resistivity, the perturbed growth rates grow as $\alpha \propto \eta^{1/3}$; however, as the resistivity increases to a certain value, the growth rate becomes independent of the resistivity and reproduces the classical growth rate in ideal fluids. In short, the magnetic field is diffused by the resistivity to enhance the instability, and the perturbed growth rates reproduce the classical growth rates, independent of the resistivity η_2.

IV. CONCLUSIONS AND REMARKS

In this paper, we perform a revised analysis of Jukes' derivation regarding the dispersion relation of MRT instability in magnetohydrodynamics with finite resistivity. We identify an erroneous boundary condition that was previously employed to ensure continuity of magnetic stress which is physically incorrect and conflicts with Chandrasekhar's theory. To obtain an accurate dispersion relation, we use a correct boundary condition. Our findings reveal interesting physical insights.

The impact of larger growth rates on the magnetic field can lead to rapid diffusion, which in turn can weaken the

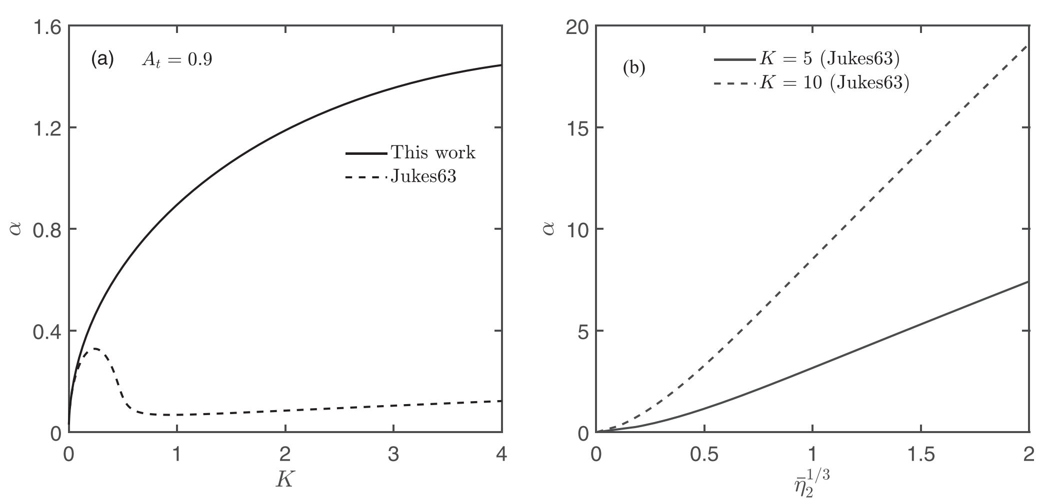

FIG. 5. (a) Growth rates σ given by this work and by Jukes as a function of K with $A_t = 0.9$. (b) Growth rates σ given by Jukes as a function of $\eta_2^{1/3}$ with $K = 5$ and $K = 10$.

suppressive effects attributed to horizontal magnetic fields. Hence, the Atwood number may significantly influence the growth-rate curves, while a self-similarity is evident in the growth-rate curves derived by Jukes'. Our findings demonstrate that long wavelengths grow at a rate proportional to $\alpha \propto \eta^{1/3}$, and under sufficiently large resistivity, growth rates tend to stabilize at a constant value, once the suppressive effect of the magnetic field fades away. However, such characteristics are absent in Jukes' theory. For instance, consider the physical parameters of hot plasma in high-energy-density physics, where the acceleration is $g \sim 10^{13}$ m/s^2 [45], the magnetic-flux-density intensity is $B \sim 100$ T, the fuel density of the capsule is $\rho \sim 1$ g/cm^3, the resistivity is between $\eta \sim 10^{-5}$ and 10^{-3} kg m^3 S^{-3} A^{-2} [46], the magnetic permeability is approximately $\mu_0 \sim 10^{-1}$ H/m, and the typical plasma temperature is $\sim 10^4$ K. Therefore, the dimensionless parameter $\bar{\eta} = \frac{\eta g}{V^3} = \frac{\eta g \rho_2^{3/2}}{\mu_0^{3/2}(B_x/\mu_0)^3} \sim 10^6$, which indicates that the MRT instability remains unaffected by the presence of the magnetic field.

We investigate the MRT instability in magnetohydrodynamics with finite resistivity in the presence of a horizontal magnetic field. Our study demonstrates that the outcomes associated with Atwood number, resistivity, and diffusion vary markedly from Jukes' results. Additionally, recent experiments indicate that Spitzer's model may significantly underestimate plasma conductivity in high-energy-density regimes. Our straightforward analytical theory has the potential to become a benchmark for comprehending plasma resistivity under extreme conditions.

ACKNOWLEDGMENTS

This work has been supported by the National Natural Science Foundation of China (Grants No. 12372353 and No. 12141201).

APPENDIX

In this paper, we construct the coupled equations of the piston and the shock to describe their coupled dynamics by assuming that the shock wave is strong enough, in order to solve the above-mentioned equations analytically. Once the asymptotic behavior of the strong shock has been obtained, the results about the weak shock wave are complementary to clarify the attenuation and decay of the shock wave of medium strength.

Therefore, considering the flows with finite conductivity, we have the following component forms of the perturbed magnetic fields,

$$\frac{\partial h_x}{\partial t} = H_x \frac{\partial u_x}{\partial x} + \eta \nabla^2 h_x, \tag{A1}$$

$$\frac{\partial h_z}{\partial t} = H_x \frac{\partial u_z}{\partial x} + \eta \nabla^2 h_z, \tag{A2}$$

where η is the resistivity of the plasma. The resistivity can be expressed as

$$\eta = \frac{1}{\sigma \mu_0}. \tag{A3}$$

Taking Eqs. (6)–(8) in Eq. (4), the equation of motion explicitly shows

$$\frac{\partial u_i}{\partial t} - \frac{\mu_0 H_j}{4\pi\rho}\frac{\partial H_i}{\partial x_j} = -\frac{\partial}{\partial x_i}\left(\frac{p}{\rho} + \mu_0 \frac{|\mathbf{H}|^2}{8\pi\rho}\right) + g, \tag{A4}$$

where $i, j = 1, 2$ represent the x and z directions. Here, we follow the previous treatments of Helmholtz's decomposition theorem by assuming that the velocity field is the sum of an irrotational part plus a solenoidal part. They are determined by the scalar potential ϕ and the vector potential $\boldsymbol{\psi}$, respectively:

$$\mathbf{u} = \nabla\phi + \nabla \times \boldsymbol{\psi}. \tag{A5}$$

To meet the requirement of incompressibility, the velocity field along the x and z directions is normally written as

$$u_x = \frac{\partial \phi}{\partial x} - \frac{\partial \psi}{\partial z}, \quad u_z = \frac{\partial \phi}{\partial z} + \frac{\partial \psi}{\partial x}, \tag{A6}$$

where ϕ satisfies the Laplace equation by using Eq. (A6) in Eq. (3), and ψ can be determined by taking the curl of Eq. (A4), leading to the vorticity equation

$$\frac{\partial \boldsymbol{\Omega}}{\partial t} = \mu_0 \frac{H_x}{\rho}\left(\frac{\partial^2 h_z}{\partial x^2} + \frac{\partial^2 h_z}{\partial z^2}\right), \tag{A7}$$

where $\boldsymbol{\Omega} = \nabla \times \mathbf{u} = \nabla^2 \boldsymbol{\psi}$ is the vorticity generated in a conducting fluid with finite resistivity. Interestingly, without considering the finite resistivity, no vorticity is generated due to the presence of a horizontal magnetic field in the linear analysis [18]. When either a horizontal or vertical magnetic field exists, vorticity travels away from the interface at the local Alfvén velocity by considering the vorticity generated by the perturbed interfaces [22,23]. As done in previous treatments, the velocity potential and stream function are defined as

$$\phi_i = A_i e^{\pm kz + nt} e^{ikx}, \quad \psi_i = B_i e^{q_i z + nt} e^{ikx}, \tag{A8}$$

where $\pm k$ with $k = 2\pi/\lambda$ denotes the decay modes with which the velocity of the irrotational part must vanish for $z \to \infty$ in both flows, and λ indicates the wavelength of the perturbation. q is the decay mode determined by the presence of a horizontal magnetizing field; when considering the resistivity, it reads

$$m_i^2 = k^2 + \frac{\mu_0 n}{\eta} + \frac{\mu_0^2 H_x^2 k^2}{\rho_i \eta}, \tag{A9}$$

which recovers Jukes' expressions for the decay modes [42]. The detailed information of the velocity field is known once the decay modes are established. The dispersion relation is obtained by using the continuities of velocities and stress tensors along the x and z directions, which have been used extensively and read

$$u_{1z} = u_{2z}, \quad h_{1x} = h_{2x}, \quad h_{1z} = h_{2z}, \quad S_{1zz} = S_{2zz}, \tag{A10}$$

where S_{ij} is the stress tensor given by

$$S_{ij} = T_{ij} - P\delta_{ij}, \tag{A11}$$

and T_{ij} is the magnetic stress tensor, which reads

$$T_{ij} = (H_i H_j - \delta_{ij} H^2/2), \tag{A12}$$

where δ_{ij} is Kronecker's delta.

[1] Y. Zhou, Phys. Rep. **720-722**, 1 (2017).
[2] Y. Zhou, Phys. Rep. **723-725**, 1 (2017).
[3] Y. Zhou, T. T. Clark, D. S. Clark, S. Gail Glendinning, M. Aaron Skinner, C. M. Huntington, O. A. Hurricane, A. M. Dimits, and B. A. Remington, Phys. Plasmas **26**, 080901 (2019).
[4] Y. Zhou, R. J. Williams, P. Ramaprabhu, M. Groom, B. Thornber, A. Hillier, W. Mostert, B. Rollin, S. Balachandar, P. D. Powell, A. Mahalov, and N. Attal, Physica D **423**, 132838 (2021).
[5] J. J. Hester, Annu. Rev. Astron. Astrophys. **46**, 127 (2008).
[6] S. A. Piriz, A. R. Piriz, and N. A. Tahir, Phys. Fluids **30**, 111703 (2018).
[7] S. A. Piriz, A. R. Piriz, and N. A. Tahir, J. Fluid Mech. **867**, 1012 (2019).
[8] D. B. Sinars, S. A. Slutz, M. C. Herrmann, R. D. McBride, M. E. Cuneo, K. J. Peterson, R. A. Vesey, C. Nakhleh, B. E. Blue, K. Killebrew, D. Schroen, K. Tomlinson, A. D. Edens, M. R. Lopez, I. C. Smith, J. Shores, V. Bigman, G. R. Bennett, B. W. Atherton, M. Savage *et al.*, Phys. Rev. Lett. **105**, 185001 (2010).
[9] S. A. Slutz, M. C. Herrmann, R. A. Vesey, A. B. Sefkow, D. B. Sinars, D. C. Rovang, K. J. Peterson, and M. E. Cuneo, Phys. Plasmas **17**, 056303 (2010).
[10] P. Y. Chang, G. Fiksel, M. Hohenberger, J. P. Knauer, R. Betti, F. J. Marshall, D. D. Meyerhofer, F. H. Séguin, and R. D. Petrasso, Phys. Rev. Lett. **107**, 035006 (2011).
[11] M. R. Gomez, S. A. Slutz, A. B. Sefkow, D. B. Sinars, K. D. Hahn, S. B. Hansen, E. C. Harding, P. F. Knapp, P. F. Schmit, C. A. Jennings, T. J. Awe, M. Geissel, D. C. Rovang, G. A. Chandler, G. W. Cooper, M. E. Cuneo, A. J. Harvey-Thompson, M. C. Herrmann, M. H. Hess, O. Johns *et al.*, Phys. Rev. Lett. **113**, 155003 (2014).
[12] D. H. Barnak, J. R. Davies, R. Betti, M. J. Bonino, E. M. Campbell, V. Y. Glebov, D. R. Harding, J. P. Knauer, S. P. Regan, A. B. Sefkow, A. J. Harvey-Thompson, K. J. Peterson, D. B. Sinars, S. A. Slutz, M. R. Weis, and P.-Y. Chang, Phys. Plasmas **24**, 056310 (2017).
[13] C. A. Walsh, K. McGlinchey, J. K. Tong, B. D. Appelbe, A. Crilly, M. F. Zhang, and J. P. Chittenden, Phys. Plasmas **26**, 022701 (2019).
[14] J. D. Moody, B. B. Pollock, H. Sio, D. J. Strozzi, D. D.-M. Ho, C. A. Walsh, G. E. Kemp, B. Lahmann, S. O. Kucheyev, B. Kozioziemski, E. G. Carroll, J. Kroll, D. K. Yanagisawa, J. Angus, B. Bachmann, S. D. Bhandarkar, J. D. Bude, L. Divol, B. Ferguson, J. Fry *et al.*, Phys. Rev. Lett. **129**, 195002 (2022).
[15] C. A. Walsh, R. Florido, M. Bailly-Grandvaux, F. Suzuki-Vidal, J. P. Chittenden, A. J. Crilly, M. A. Gigosos, R. C. Mancini, G. Pérez-Callejo, C. Vlachos, C. McGuffey, F. N. Beg, and J. J. Santos, Plasma Phys. Control. Fusion **64**, 025007 (2022).
[16] C. Walsh, A. Crilly, and J. Chittenden, Nucl. Fusion **60**, 106006 (2020).
[17] E. C. Hansen, J. R. Davies, D. H. Barnak, R. Betti, E. M. Campbell, V. Y. Glebov, J. P. Knauer, L. S. Leal, J. L. Peebles, A. B. Sefkow, and K. M. Woo, Phys. Plasmas **27**, 062703 (2020).
[18] S. Chandrasekhar, *Hydrodynamic and Hydromagnetic Stability* (Dover, New York, 1981)
[19] B. Srinivasan and X.-Z. Tang, Phys. Plasmas **20**, 056307 (2013).
[20] A. Bose, J. Peebles, C. A. Walsh, J. A. Frenje, N. V. Kabadi, P. J. Adrian, G. D. Sutcliffe, M. Gatu Johnson, C. A. Frank, J. R. Davies, R. Betti, V. Y. Glebov, F. J. Marshall, S. P. Regan, C. Stoeckl, E. M. Campbell, H. Sio, J. Moody, A. Crilly, B. D. Appelbe *et al.*, Phys. Rev. Lett. **128**, 195002 (2022).
[21] T. Sano, T. Inoue, and K. Nishihara, Phys. Rev. Lett. **111**, 205001 (2013).
[22] V. Wheatley, R. Samtaney, and D. I. Pullin, Phys. Fluids **21**, 082102 (2009).
[23] V. Wheatley, R. Samtaney, D. I. Pullin, and R. M. Gehre, Phys. Fluids **26**, 016102 (2014).
[24] B.-I. Jun, M. L. Norman, and J. M. Stone, Astrophys. J. **453**, 332 (1995).
[25] M. J.-E. Manuel, A. B. Sefkow, C. C. Kuranz, A. M. Rasmus, S. R. Klein, M. J. MacDonald, M. R. Trantham, J. R. Fein, P. X. Belancourt, R. P. Young, P. A. Keiter, B. B. Pollock, J. Park, A. U. Hazi, G. J. Williams, H. Chen, and R. P. Drake, Phys. Rev. Lett. **122**, 225001 (2019).
[26] M. J.-E. Manuel, B. Khiar, G. Rigon, B. Albertazzi, S. R. Klein, F. Kroll, F. E. Brack, T. Michel, P. Mabey, S. Pikuz, J. C. Williams, M. Koenig, A. Casner, and C. C. Kuranz, Matter Radiat. Extremes **6**, 026904 (2021).
[27] Y. T. Lee and R. M. More, Phys. Fluids **27**, 1273 (1984).
[28] R. S. Cohen, L. Spitzer, and P. M. Routly, Phys. Rev. **80**, 230 (1950).
[29] Z. Barbeau, K. Raman, M. Manuel, S. Nagel, and B. Shivamoggi, Phys. Plasmas **29**, 012306 (2022).
[30] R. K. Bera, Y. Song, and B. Srinivasan, J. Plasma Phys. **88**, 905880209 (2022).
[31] Y. Song and B. Srinivasan, Radiat. Eff. Defects Solids **175**, 1009 (2020).
[32] B. K. Shivamoggi, Phys. Scr. **24**, 49 (1981).
[33] C. R. Weber, A. W. Cook, and R. Bonazza, J. Fluid Mech. **725**, 372 (2013).
[34] C. R. Weber, D. S. Clark, A. W. Cook, L. E. Busby, and H. F. Robey, Phys. Rev. E **89**, 053106 (2014).
[35] P. F. Valézquez, D. O. Gómez, G. M. Dubner, G. Giménez de Castro, and A. Costa, Astron. Astrophys. **334**, 1060 (1998).
[36] D. Capelli, D. W. Schmidt, T. Cardenas, G. Rivera, R. B. Randolph, F. Fierro, E. C. Merritt, K. A. Flippo, F. W. Doss, and J. L. Kline, Fusion Sci. Technol. **70**, 316 (2016).
[37] E. C. Harding, J. F. Hansen, O. A. Hurricane, R. P. Drake, H. F. Robey, C. C. Kuranz, B. A. Remington, M. J. Bono, M. J. Grosskopf, and R. S. Gillespie, Phys. Rev. Lett. **103**, 045005 (2009).
[38] Y. B. Sun and C. Wang, Phys. Rev. E **101**, 053110 (2020).
[39] C. A. Walsh, Phys. Rev. E **105**, 025206 (2022).
[40] K. Matsuo, T. Sano, H. Nagatomo, T. Somekawa, K. F. F. Law, H. Morita, Y. Arikawa, and S. Fujioka, Phys. Rev. Lett. **127**, 165001 (2021).
[41] C. A. Walsh and D. S. Clark, Phys. Rev. E **107**, L013201 (2023).
[42] J. D. Jukes, J. Fluid Mech. **16**, 177 (1963).
[43] J. M. Stone and T. Gardiner, Astrophys. J. **671**, 1726 (2007).
[44] R. P. Drake, *High-Energy-Density Physics. Fundamentals, Inertial Fusion, and Experimental Astrophysics* (Springer, Berlin, 2013).
[45] G. A. Wurden, S. C. Hsu, T. P. Intrator, T. C. Grabowski, J. H. Degnan, M. Domonkos, P. J. Turchi, E. M. Campbell, D. B. Sinars, M. C. Herrmann, R. Betti, B. S. Bauer, I. R. Lindemuth, R. E. Siemon, R. L. Miller, M. Laberge, and M. Delage, J. Fusion Energy **35**, 69 (2016).
[46] Z. Fu, L. Jia, X. Sun, and Q. Chen, High Energy Density Phys. **9**, 781 (2013).